In situ Activation of Bimetallic Pd–Pt Methane Oxidation Catalysts

Kyle A. Karinshak[+],[a, b] Patrick Lott[+],[a] Michael P. Harold,*[b] and Olaf Deutschmann*[a]

This study investigates possible pathways to reduce water inhibition over Pd–Pt methane oxidation catalysts supported on alumina and a ceria-zirconia mixed oxide under conditions typical for lean burn gas engines. Spatially resolved concentration and temperature profiles reveal that addition of hydrogen to the lean reaction mixture leads to significant heat production and an increase in methane conversion. Moreover, reductive pulses during operation are not only able to regenerate the catalyst deactivated by water by removal of OH-groups from the catalyst surface, but even promote its activity after repeated application of pulsing for several hours. X-ray absorption spectroscopy reveals the formation of a partially reduced PdO–Pd mixture during the pulsing, which explains the increase in activity. This state of high activity is stable for several hours under the tested lean conditions. The results presented in this study suggest an efficient *in situ* activation strategy to overcome water inhibition of methane total oxidation over Pd–Pt catalysts by careful process control.

Introduction

Natural gas engines may increasingly replace diesel and gasoline engines due to the ubiquity of natural gas as fuel and the lower CO_2 and particulate matter emissions resulting from natural gas combustion. Unfortunately, a small amount of methane always remains after combustion. As CH_4 is a much more potent greenhouse gas than CO_2, this CH_4 slip – as much as several hundred ppm depending on the vehicle operation – may become a significant obstacle to the widespread use of natural gas as a transportation fuel.[1] Therefore, an efficient after-treatment system must be able to abate this remaining methane. This is a challenge for both, lean combustion and stoichiometric combustion; in the case of the latter the Three-Way Catalyst (TWC) is largely ineffective.[2]

The typical lean-burn engine exhaust has several challenging obstacles for effective catalytic methane oxidation. The engine exhaust stream is highly lean (up to approximately 10% O_2), contains significant amounts of water (up to 12–15 vol.%), contains SO_x (fuel source dependent) and has only moderate temperatures (typically below 500 °C).[3] Supported platinum group metals (PGM) are the favored active catalytic components for the treatment of methane under these conditions, with Pd-based catalysts showing the highest activity.[3,4] Under lean conditions, the active state of Pd is believed to be PdO, although there is an ongoing debate as to whether other phases of Pd or a combination of phases could be more active.[5–17] In addition to PGM loading, the catalytic activity is affected by the catalyst support, metal dispersion, gas environment and even operating history.[18–23] Bimetallic catalysts, wherein a small amount of Pd is replaced with Pt, have been found to be more active, more hydrothermally stable and sintering resistant, and possess somewhat higher sulfur resistance compared to monometallic Pd catalysts.[24–31] Furthermore, research by *Epling and Hoflund* has shown that mixtures of Pd^0 and PdO are more catalytically active than pure PdO, presumably due to facilitated CH_4 dissociation on metallic Pd.[32] Recent work by *Chin et al.* shows that the site pair Pd-PdO is effective for CH_4 dissociation to CH_3 and OH.[33]

Despite the improved performance from the addition of Pt, inhibition from water vapor and sulfur compounds still pose significant challenges. Water vapor inhibits catalytic activity through competitive adsorption with methane as well as deactivation through formation and accumulation of surface hydroxyl species.[34–37]

Previous research has shown that brief reductive periods during lean operation of Pd-based catalysts can not only regenerate catalysts deactivated by water or sulfur compounds, but can also stabilize their catalytic performance above what it would otherwise be.[18,22,38,39] Similarly, *Petrov et al.* applied periodic rich phases to continuously regenerate a Pd/zeolite catalyst for lean methane oxidation.[40] In the context of methane abatement in the exhaust of a natural gas engine by a TWC, *Bounechada et al.* similarly found that periodic rich pulses could recover catalytic activity lost due to water inhibition and that periodic oscillations resulted in higher and more stable catalytic methane conversion over a Pd/Rh-based TWC.[41]

[a] *K. A. Karinshak,[+] P. Lott,[+] Prof. Dr. O. Deutschmann*
Institute for Chemical Technology and Polymer Chemistry (ITCP)
Karlsruhe Institute of Technology (KIT)
Engesserstr. 20
76131 Karlsruhe (Germany)
E-mail: deutschmann@kit.edu
[b] *K. A. Karinshak,[+] Prof. Dr. M. P. Harold*
Department of Chemical and Biomolecular Engineering
University of Houston
4726 Calhoun Rd
Houston TX 77204-4004 (USA)
E-mail: mharold@uh.edu
[+] *These authors contributed equally to this work.*

Supporting information for this article is available on the WWW under https://doi.org/10.1002/cctc.202000603

Despite some references to the beneficial effects of reductive regenerative periods on Pd-based methane oxidation catalysts that have been deactivated by water in a lean environment,[22,40,42] to our knowledge there has been no substantial systematic investigation on the potential effects and underlying mechanisms by which reductive pulses can benefit lean methane oxidation.

Starting from a broad data set of systematic fundamental experiments, this study presents a method for *in situ* activation of Pd–Pt/Al_2O_3 and Pd–Pt/CeO_2–ZrO_2–Y_2O_3–La_2O_3 (in the following referred to as Pd–Pt/CZ) methane oxidation catalysts under different temperatures and gas compositions. Specifically, periodic reductive pulses of hydrogen are demonstrated to result in two distinct effects dependent upon the operating conditions. Further knowledge of the processes on the catalysts were gained by spatial profiling of the gas species concentrations and gas phase temperature using a capillary technique. With our study we aim at contributing to more efficient low-temperature methane oxidation over Pd-based catalysts and understanding the factors governing high catalytic activity.

Results and Discussion

Light-off trends at varying feed composition. Figure 1 compares the light-off curves for Pd–Pt/CZ (Figure 1a) and Pd–Pt/Al_2O_3 (Figure 1b) in feeds with different combinations of H_2O and H_2 after oxidative pretreatment (1 h in 10% O_2, bal. Ar at 550 °C). For the Pd–Pt/CZ catalyst under baseline operating conditions (A) – no H_2O or H_2 in the feed – the light-off temperature is ~360 °C and complete CH_4 conversion is achieved at 450 °C. The addition of water to the feed (B) has a well-known significant inhibitory effect on the catalytic activity,[9,37,43] increasing T_{50} by ~100 °C and the complete conversion temperature to ~550 °C. This is a result of surface hydroxyl formation on top and at the periphery of the noble metal particles, possibly in the form of $Pd(OH)_2$.[44] These hydroxylated sites are considered catalytically inactive.[36,37]

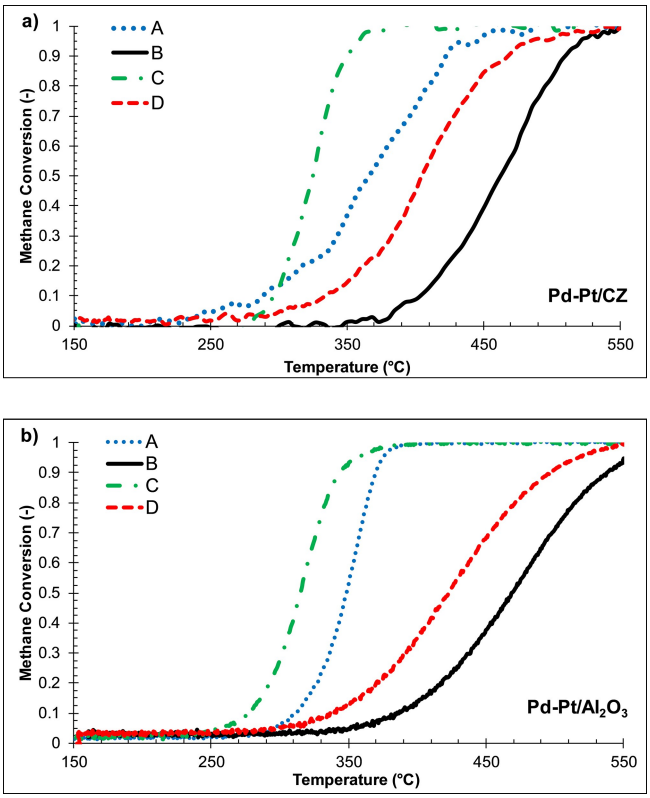

Figure 1. Light-off curves of **a)** Pd–Pt/CZ and **b)** Pd–Pt/Al_2O_3 in 10% O_2, 2000 ppm CH_4 and bal Ar (A), A plus 12% H_2O (B), A plus 1% H_2 (C), and A plus 12% H_2O and 1% H_2 (D).

Addition of 1% H_2 to the feed promotes CH_4 oxidation. The conversion obtained with the feed containing H_2 (curve C) has a T_{50} of 325 °C and a complete conversion temperature of 380 °C. Note that at lower temperatures (< 300 °C) the feed with H_2 has a slightly lower CH_4 conversion. This may be a result of inhibition by the water generated from H_2 oxidation, resulting in blockage of active sites. When H_2O and H_2 are present (D), T_{50} decreased by 60 °C from that of the wet feed without H_2 (B). This is attributed to a temperature increase from the exothermic H_2 oxidation. The same general trends were also observed for the Pd–Pt/Al_2O_3 catalyst (Figure 1b). For this catalyst, the addition of H_2 results in a T_{50} 35 °C lower compared to dry conditions and 45 °C lower under wet conditions.

To examine the impact of H_2 in more detail, light-off experiments for different concentrations of H_2 in the presence of water were conducted. The dry feed with 1% H_2 is provided for comparison (Figure 2). The general trend is a shift of the light-off curves to the left with the addition of H_2. It is interesting to note the rather insensitive dependence of the CH_4 conversion on H_2 concentration between 0.2% and 2% for the wet feed. However, by 5% the light-off curve shifts sharply to lower temperature. This nonlinear dependence of the CH_4 conversion on the H_2 concentration is caused by competition between the beneficial impact of heat generation and the detrimental impact of hydroxyl formation. Moreover, there is a shift from the typical sigmoidal shape at low H_2 feed concentrations to an unusual convex curve when 5% H_2 are

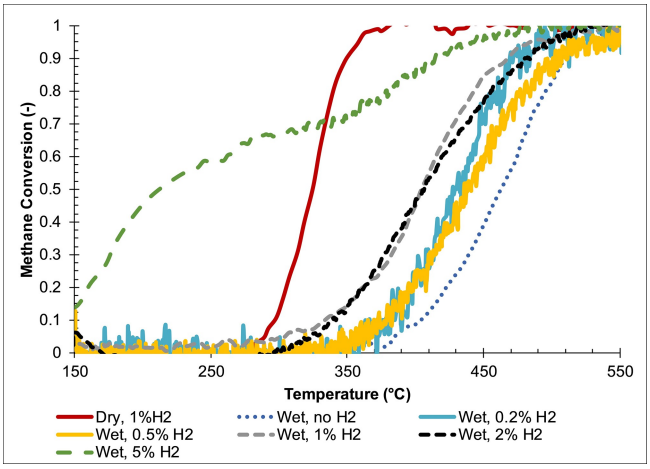

Figure 2. Light-off curves of Pd–Pt/CZ in 10% O_2, 2000 ppm CH_4, bal. Ar, and (if wet) 12% H_2O under increasing concentrations of H_2.

added. This conveys the much lower activation energy for H_2 oxidation compared to CH_4 oxidation.

Spatially resolved species concentration and temperature profiles (so-called spatial profiling, hereinafter mentioned as SpaciPro) provide further insight. Figure 3 shows the concentration measurements along the catalyst. When O_2 is present, CH_4 is completely oxidized to CO_2 and no CO was detected during these experiments. SpaciPro measurements under steady state conditions consistently suggest that only minor amounts of H_2 reach the front heat shield (FHS, used to minimize temperature gradients) zone or the catalyst itself. Similar behavior was observed for the Pd–Pt/CZ catalyst. In one light-off experiment, the capillary connected to the mass spectrometer (MS) was placed in-between the FHS and the catalyst. According to the MS data, 94% of the H_2 reacted with oxygen before it reached the catalyst; as the temperature increased this value approached 99%. The remaining H_2 was quickly converted to water upon contact with the catalysts.

This behavior is attributed to a combination of effects. With its small size, H_2 is able to back-diffuse against the convective current, which can potentially lead to apparent pre-catalyst consumption due to mixing. In addition, the MS settings could cause a reaction of H_2 with O_2 inside the ionization chamber, which may result in misleading high H_2 conversion. Thus, it is likely that H_2 reaches the catalyst but cannot be detected due to experimental hurdles. As H_2 oxidation is a highly exothermic reaction, the temperature profiles discussed later clarify this open question and confirm that H_2 in fact is converted at the catalyst inlet.

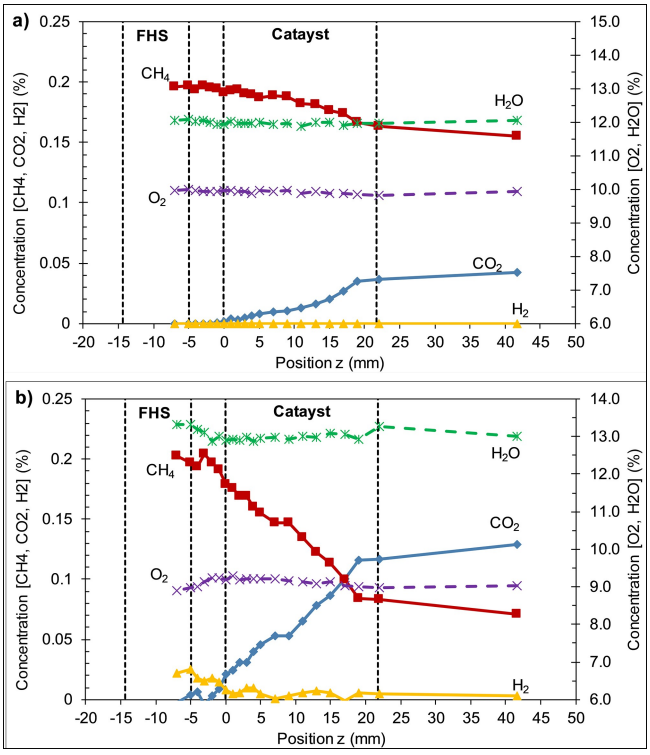

Figure 3. SpaciPro results for Pd–Pt/Al_2O_3 in **a)** 10% O_2, 2000 ppm CH_4, 12% H_2O, and bal. Ar at 430 °C and **b)** 10% O_2, 2000 ppm CH_4, 1% H_2, 12% H_2O, and bal. Ar at 430 °C.

The presence of H_2 affects the catalyst during both pretreatment and operation. Discussed in more detail in the following section, spatial temperature measurements during transient operation show a significant temperature rise as a result of the exothermic oxidation of H_2. This in turn leads to an increase in CH_4 oxidation rate. That the relationship between H_2 feed concentration and CH_4 oxidation light-off is nonlinear underscores contributions from the reaction exothermicity and the aforementioned sensitivity to H_2O.

The enhancement in light-off behavior due to the reductive pretreatments may be ascribed to separate interactions between H_2 and the support and Pd complexes. *Bozo et al.* showed that CZ plays an active role in CH_4 oxidation, augmenting the supply of oxygen.[20] Reductive pretreatments of H_2 were shown to create surface oxygen vacancies in the CZ, allowing electron transfer to the Pd and resulting in higher catalytic activity. *Xiong et al.* and *Mahara et al.* reported that reductive treatments of PdO complexes resulted in the formation of metastable PdO–Pd^0 domains which are more active for CH_4 oxidation.[5,45]

Effect of pulses: continuous O_2 stream while pulsing H_2. The catalysts were exposed to pulses of H_2, with all other gases kept constant, for the duration of the SpaciPro measurements. Figure 4 shows the CH_4 conversion and effluent temperature for Pd–Pt/CZ under steady-state operation and during H_2 pulses for dry and wet conditions.

For a dry feed, introduction of 1% H_2 results in an initial decrease in conversion due to the H_2O generation and its subsequent adsorption. For a wet feed, the additional water generated by the H_2 oxidation has little effect. As discussed above in the context of Figure 3, most of the H_2 appeared to be converted before reaching the catalyst during steady-state operation. The MS data suggest a similar behavior during H_2 pulsing experiments. SpaciPro temperature probes show the temperature at the front of the catalyst by 85 °C higher during the 1% H_2 pulse, regardless of initial catalyst temperature or the absence/presence of water. The measured temperature rise, evident in Figure 5, points to the fact that most of the H_2 reaches the monolith, in contrast to the concentration profile obtained from evaluation of the SpaciPro data. The temperature increase during H_2 pulsing leads to a cycle average increase in the CH_4 conversion under 2% and 3% H_2 pulses, and no net change for the 1% pulses. In all cases, the H_2 pulsing is unable to prevent the long-term decline in the CH_4 conversion over several hours.

The temporal profiles of CH_4 conversion and effluent temperature during 30 s/180 s H_2 pulsing over Pd–Pt/CZ at three different H_2 feed concentrations reveal an initial conversion decrease of ~15–20% during the 30 s H_2 pulse followed by a sharp 30–40% increase just after the pulse (Figure S7). The CH_4 conversion decrease encountered during the H_2 pulse is attributed to the nearly instantaneous inhibition of CH_4 oxidation by H_2O produced from H_2 oxidation. Afterwards, the effluent temperature increases during the 180 s H_2-off period, attributed to the heat generated by the exothermic H_2

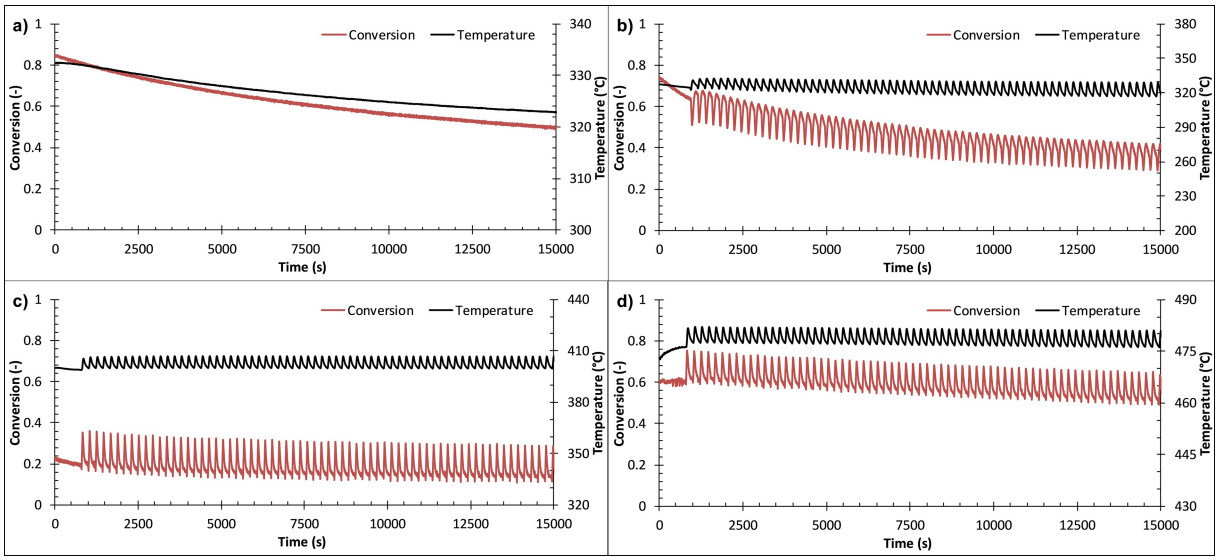

Figure 4. Effluent CH_4 conversion and temperature for Pd–Pt/CZ under various conditions. **a)** Steady-state 10% O_2, 2000 ppm CH_4, bal. Ar at 315 °C. **b)** 10% O_2, 2000 ppm CH_4, bal. Ar with 30 s/180 s on/off pulses of H_2 at 315 °C. **c)** 10% O_2, 12% H_2O, 2000 ppm CH_4, bal. Ar with 30 s/180 s on/off pulses of H_2 at 400 °C. **d)** 10% O_2, 12% H_2O, 2000 ppm CH_4, bal. Ar with 30 s/180 s on/off pulses of H_2 at 470 °C.

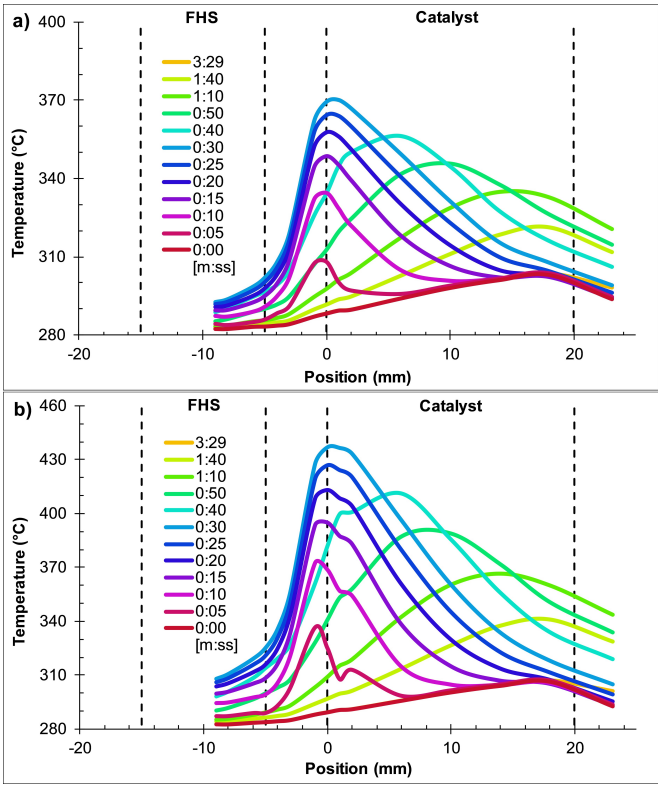

Figure 5. Temporal evolution of the spatially resolved temperature profiles during H_2 pulses of **a)** 1% H_2 and **b)** 2% H_2 over a Pd–Pt/Al_2O_3 catalyst. Experiments carried out in 10% O_2, 2000 ppm CH_4, bal. Ar with 30 s/180 s on/off pulses of H_2 at 295 °C. H_2 is in the system for the first 30 s.

oxidation propagating down the catalyst. Effluent temperatures (Figure 5) reach a maximum 40 s after the end of the H_2 pulse, consistent with the effluent temperature profiles in Figure S7b.

As previously stated, spatial temperature profiles for the 1% and 2% H_2 feed concentrations explain the effects of H_2 pulsing. The initial temperature profile (time = 0 s, before H_2 pulse initiation) shows that the temperature increases along the monolith length due to the incomplete conversion of CH_4. Over the next 30 s the pulsed H_2 oxidizes and results in a dramatic temperature increase at the front of the monolith. A maximum temperature rise of ~85 °C is observed for the 1% H_2 pulse while a ~155 °C increase is encountered when pulsing 2% H_2. After the H_2 pulse ends, the heat diffuses down the catalyst. The heat from H_2 oxidation remains well after the produced H_2O, resulting in the temporary boost to CH_4 oxidation. With respect to the experimental data shown in Figure 3b, the temporal temperature increase around the catalyst inlet (Figure 5) that originates form the high exothermicity of the H_2 oxidation clearly indicates that H_2 actually reaches the catalyst and is not consumed before.

Effect of pulses: switching between O_2 and H_2 streams. Alternating between O_2 and H_2 pulses has a dramatic effect on catalytic performance. Figure 6 shows the CH_4 conversion for Pd–Pt/CZ over a period of about 4 h during lean-rich (O_2/H_2) pulsing. Figures 6a and 6b correspond to a dry feed carried out at 295 °C and 315 °C, respectively. The experiments demonstrate the sustained CH_4 conversion achieved with the H_2/O_2 pulsing, in contrast to the gradual conversion decline over the same period for the H_2 pulsing in a constant 10% O_2 (Figure 4). At 290 °C (Figure 6a) the conversion is sustained at ~5–22% from its ~30% initial level while at 315 °C (Figure 6b) the conversion is sustained at ~5–70% from its ~60% initial level.

Under wet conditions, H_2/O_2 pulses result in sustained, boosted catalyst activity. At 400 °C (Figure 6c) the conversion is sustained at ~30–70% from its ~40% initial level while at 430 °C (Figure 6b) the conversion is sustained at ~70–95% from

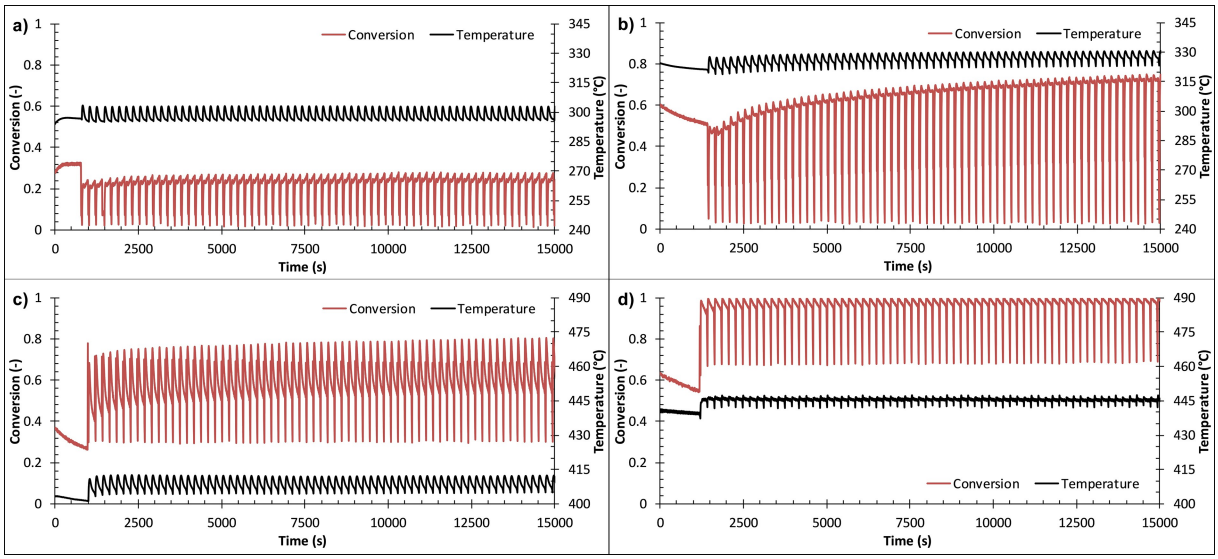

Figure 6. Effluent CH_4 conversion and temperature for Pd–Pt/CZ under various conditions. **a)** 2000 ppm CH_4, bal. Ar with 30 s/180 s of 1% H_2/10% O_2 at 290 °C. **b)** 2000 ppm CH_4, bal. Ar with 30 s/180 s of 1% H_2/10% O_2 at 315 °C. **c)** 12% H_2O, 2000 ppm CH_4, bal. Ar with 30 s/180 s of 1% H_2/10% O_2 at 400 °C. **d)** 12% H_2O, 2000 ppm CH_4, bal. Ar with 30 s/180 s of 1% H_2/10% O_2 at 430 °C.

its ~60% initial level. Similar results were obtained for Pd–Pt/Al_2O_3 (Figure S8).

Spatially resolved temperature profiles shown in Figure 7 for the 315 °C dry feed experiment reveal temperature changes along the catalyst bed consistent with the slowing and accelerating of the CH_4 oxidation reaction. Between 0 s and 30 s, H_2 is admitted while between 31 s and 210 s O_2 is admitted. During the H_2 feed the temperature drops due to the lack of O_2. Upon the admission of O_2 heating of the entire catalyst is observed. Unlike in the case of H_2 pulses in a constant O_2 flow for which a significant hot spot was observed in the front region, the temperature profile during H_2/O_2 pulses are much more gradual and have the same shape as the initial temperature profile.

A more detailed look at the CH_4 conversion and effluent monolith temperature for the 315 °C dry-feed and 400 °C wet-feed experiments (Figure S9) reveals additional information. For the dry feed experiment the initial decrease in conversion is likely due to the rapid consumption of H_2 by stored O_2. This results in the generation of water and the rapid inhibition of CH_4 oxidation by surface hydroxyls. An even larger drop in performance quickly follows this initial decrease as gaseous O_2 is fully removed from the system and CH_4 conversion ceases. At the end of the H_2 pulse and the start of the O_2 pulse, the CH_4 conversion returns to a value slightly higher than that at the start of the cycle. Over many cycles, this slight increase in activity can result in substantial reactivation of the catalyst. More complex behavior is seen in the experiments conducted in the presence of water (Figure S9b). A brief spike in CH_4 conversion is observed when the feed is switched from lean to rich. This is followed by a steep drop in conversion as the available oxygen is consumed. Finally, as oxygen reenters the system, the conversion overshoots its value at the start of the cycle before rapidly deactivating in the lean phase.

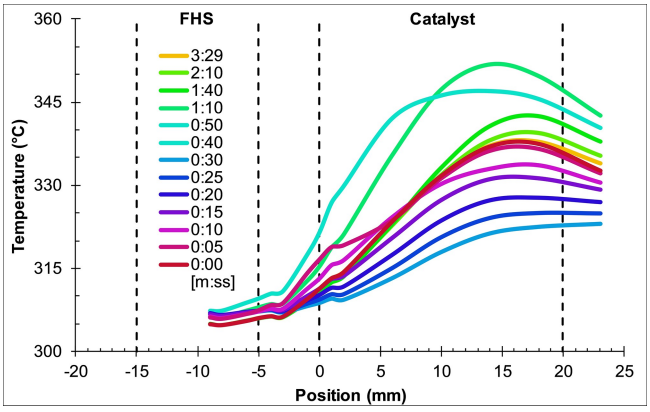

Figure 7. Temporal evolution of the spatially resolved temperature profiles during H_2/O_2 pulsing over Pd–Pt/CZ in 2000 ppm CH_4, bal. Ar and 30 s/180 s pulses of 1% H_2/10% O_2 at 315 °C.

Experiments carried out over a range of conditions indicated that the first pulse typically resulted in the largest change in the CH_4 conversion. The ultimate change depends on the initial state of the catalyst. For example, in Figure 8a, for a dry feed at 290 °C the H_2 pulse led to a sharp decrease from an initial conversion of 30% to just ~3%. Subsequent H_2/O_2 pulsing did not restore the conversion, with conversion ranging from 3–25% and a cycle-average value of 21%. Under wet conditions, the first pulse significantly raised CH_4 conversion. At 400 °C, the conversion rose from an initial value of 30% to 75% and an ultimate cycle-average value of 57% (Figure 6c). At 430 °C, the conversion jumped from 55% to 98% and a cycle-average value of 96% (Figure 6d). Again, these conversions were sustained for several hours as the catalyst remained under lean/rich switching.

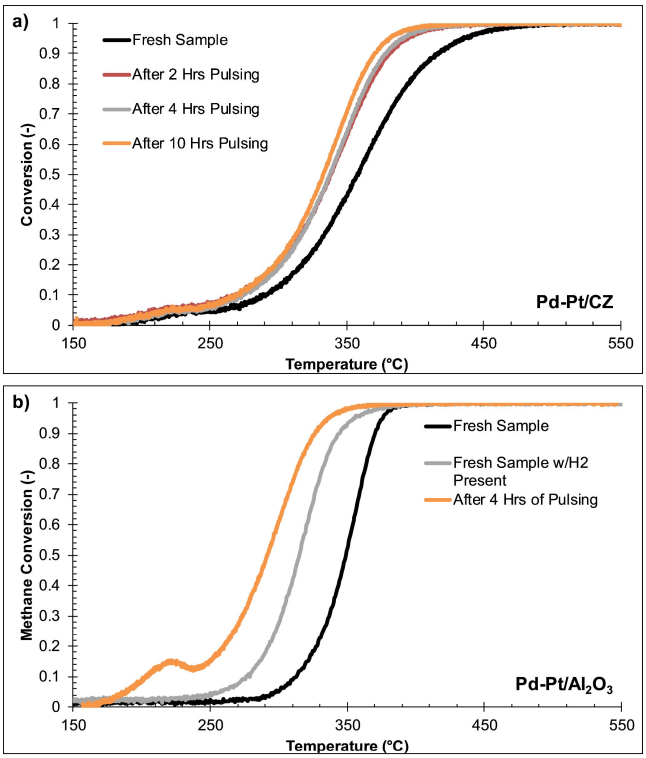

Figure 8. a) Light-off curves of Pd–Pt/CZ in 10% O_2, 2000 ppm CH_4, bal. Ar after increasing durations of H_2/O_2 pulses. **b)** Light-off curves of Pd–Pt/Al_2O_3 in 10% O_2, 2000 ppm CH_4, bal. Ar after 4 h of H_2/O_2 pulses compared to a fresh sample and a light-off profile where 1% H_2 was present.

The difference in behavior between wet and dry conditions can be explained by two competing factors. The first is the catalysts sensitivity to water. For a dry feed, the H_2O resulting from the reductive H_2 pulse inhibits CH_4 oxidation over PdO. At higher temperature the H_2 pulse is more effective in removing surface hydroxyls. The processes on the catalyst can be summarized considering the following four reactions [Eqs. (1–4)]:

$$PdO + H_2O \leftrightarrow Pd(OH)_2 \quad (1)$$

$$PdO + H_2 \leftrightarrow Pd + H_2O \quad (2)$$

$$H_2 + {}^1/_2\ O_2 \rightarrow H_2O \quad (3)$$

$$CH_4 + 2\ O_2 \rightarrow 2\ H_2O + CO_2 \quad (4)$$

For the dry feed, the only source of H_2O is the oxidation of CH_4, so the surface coverage with hydroxyls is low. The admission of H_2 leads to a large increase in the hydroxyl coverage as a result of reactions [Eq. (2)] and [Eq. (3)], which increase the H_2O concentration by H_2 oxidation, leading to the formation of hydroxyls via [Eq. (1)]. For a wet feed the already high H_2O feed concentration results in a large fraction of the surface occupied by hydroxyls. The admission of H_2 shifts the equilibrium of [Eq. (1)] to the left through the consumption of PdO in [Eq. (2)], which is more effective at higher temperature.

Carbon monoxide was observed during wet experiments (Figure S10), particularly over the Pd–Pt/Al_2O_3 catalyst. The formation of CO occurred only when the H_2 stream was engaged. CO concentration increased with increasing temperature; at 430 °C nearly 130 ppm of CO was produced during the switching pulse by the Pd–Pt/Al_2O_3 catalyst. The Pd–Pt/CZ catalyst produced only 30 ppm of CO under identical experimental conditions. Under dry conditions, CO formation was below 10 ppm if its formation was observed at all. While under highly lean conditions (10% O_2) the dominating process is the total oxidation of methane to carbon dioxide [Eq. (4)], CO formation is likely the result of steam reformation between the water and methane [Eq. (5)]:

$$CH_4 + H_2O \leftrightarrow CO + 3\ H_2 \quad (5)$$

The improvement in CH_4 oxidation performance by applying rich pulses is long-lasting and persists between experiments and after numerous pretreatments. For illustration of this observation, the catalyst was exposed to the dry conditions of the experiment in Figure 6b. After an initial decrease in the conversion to 50%, a gradual increase in conversion was observed over a several hour period of pulsing (2000 ppm CH_4, bal. Ar with 30 s/180 s of 1% H_2/10% O_2 at 315 °C). Steady state operation on the following day resulted in 15% higher initial CH_4 conversion compared to the previous day's experiment. Furthermore, it took several hours before the deactivation seen during the prior day was reached. Initial steady-state SpaciPro measurements and light-off curves showed CH_4 conversion of 20% over the Pd–Pt/CZ catalyst at 315 °C. After several experiments with O_2/H_2 switching pulses, a CH_4 conversion as high as 80% was observed.

Figure 8a shows the light off-curve of a fresh Pd–Pt/CZ catalyst and subsequent light-off curves after varying durations of H_2/O_2 switching pulses, while Figure 8b shows the behavior of the Pd–Pt/Al_2O_3 catalyst after four hours of pulsing. After 10 hours of H_2/O_2 pulsing, the Pd–Pt/CZ catalyst has experienced a 30 °C shift of the T_{50} to 330 °C. The Pd–Pt/Al_2O_3 catalyst shows an even more pronounced shift in the T_{50}, from 350 °C to 270 °C, as well as the development of a non-monotonic light-off curve. This effect has been demonstrated with H_2/O_2 pulses as short as 10 s and separated by lean-phases as long as 600 s, suggesting that the pulse duration, quantity of H_2 involved and pulse separation time can be optimized for a maximal CH_4 oxidation activity.

Our results suggest that PdO particle size/dispersion and temperature effects play a minor role and cannot explain the enhanced CH_4 oxidation in the experiments described before. Transmission electron microscopy (TEM) measurements of Pd–Pt/CZ and Pd–Pt/Al_2O_3 reveal no significant change in PGM dispersion between freshly prepared samples and samples that experienced H_2/O_2 pulsing (30 s/180 s) for 4 h at 315 °C for either catalyst (Figures S3–S5). These findings are similar to results of *Mahara et al.*:[45] Reduction of PdO/Al_2O_3 below 415 °C does not affect the particle size of PdO. The previously discussed spatial-temperature measurements of H_2/O_2 pulses (Figure 7) do not show the large exothermicity responsible for

the H_2 pulsing and steady-state effects (Figure 8). Hence, we attribute the enhanced CH_4 oxidation seen during H_2/O_2 switching results to the contributions of several, simultaneous, independent effects occurring during the reductive treatment; namely: (i) removal of accumulated hydroxyl species; (ii) formation of metastable PdO–Pd complexes; (iii) creation of oxygen vacancies in the catalyst supported on CZ. These are described next.

The inhibitory effects of hydroxyl surface species accumulation have already been discussed; removal of these species can be clearly concluded from the SpaciPro results during the H_2/O_2 pulse experiments. H_2 is observed to decrease in concentration along the length of both catalysts concurrent with the release of H_2O from the catalyst. Removal of these hydroxyl species also explains the observed brief boost in CH_4 conversion under wet conditions at 400 °C (Figure S9). By keeping water from the catalyst surface, the catalyst can briefly take advantage of the higher temperatures before O_2 completely leaves the system. That the catalysts do not lose activity over several hours under H_2/O_2 pulsing conditions implies that the rate at which H_2 removes the OH species is far faster than they can accumulate.

The second effect concerns the active metal Pd. Both *Mahara et al.* and *Xiong et al.* found that reductive conditions partially reduce PdO complexes into metastable PdO–Pd structures that were reported to show higher catalytic activity than pure PdO.[5,45] *Xiong et al.* went further and showed distinct regions of PdO and Pd on the same particle in high resolution TEM images.[5] Although we cannot see this in our TEM images, XAS spectra of Pd–Pt/CZ and Pd–Pt/Al_2O_3 samples which were pretreated by H_2/O_2 pulsing reveal reduced Pd coexisting with PdO (Figure 9). These samples were pulsed for four hours at 315 °C and were exposed to oxidizing conditions for over a minute before being cooled in Ar to room temperature. To determine the amount of metallic Pd and PdO before and after the pulse treatment, a linear combination fitting (LCF) of the Pd and PdO reference spectra was performed in the range of −20 to 30 eV around the Pd K-edge. The results obtained show that the fresh samples are fully oxidized after preparation. After pulsing, however, the fraction of metallic Pd is ~55% on Pd–Pt/Al_2O_3, while the fraction of Pd is only ~14% on Pd–Pt/CZ. Additionally, TEM revealed more pronounced alloying between the Pd and Pt on the Al_2O_3 support than on the CZ support (Figure S3). This is true not only in the fresh state, but also after H_2/O_2 pulsing (Figure S4) and is consistent with the findings of *Xiong et al.* who found that the Pt helped maintain the reduced state of Pd under oxidizing conditions.[5] We attribute the decrease in the light-off temperature of these catalysts predominantly to this effect. Furthermore, we attribute the larger improvements over the Pd–Pt/Al_2O_3 catalyst, as seen in Figure 8, to the increased amount of metallic Pd in combination with pronounced alloying between Pd and Pt. Apparently the activity can be maximized by the right Pd/PdO ratio, especially if promoted or at least stabilized by Pt. According to the found PdO/Pd ratios we can speculate, that CH_4 oxidation still takes place according to a Mars-van-Krevelen mechanism on PdO as frequently claimed.[7–9,16,17] The presence of metallic Pd may destabilize the Pd–O bond, which could ultimately result in a significant increase of the catalytic activity.

The final of the three effects concerns the Pd–Pt/CZ catalyst but not the Pd–Pt/Al_2O_3 catalyst. The reductive pulses of H_2 result in oxygen vacancies on reducible the ceria-zirconia support. *Bozo et al.* found that the CZ support played an active role in CH_4 oxidation for a Pd/CZ catalyst.[20] In the absence of gas phase oxygen, lattice oxygen was easily removed and the subsequent vacancies promoted electron transfer from the support to the Pd as well as increased lability and mobility of further lattice oxygen atoms. Hence, we can assume a similar behavior for our catalyst sample for two reasons. First, the H_2 pulses utilized in this experiment are much more reductive than the CH_4 pulses utilized by *Bozo et al.*[20] in their studies; second, SpaciPro results during pulsing revealed the release of H_2O during the reductive pulse. However, in the current study we are unable to distinguish what percentage of those released species are surface hydroxyl species and which are the result of reactions with the lattice oxygen. For this, further investigations

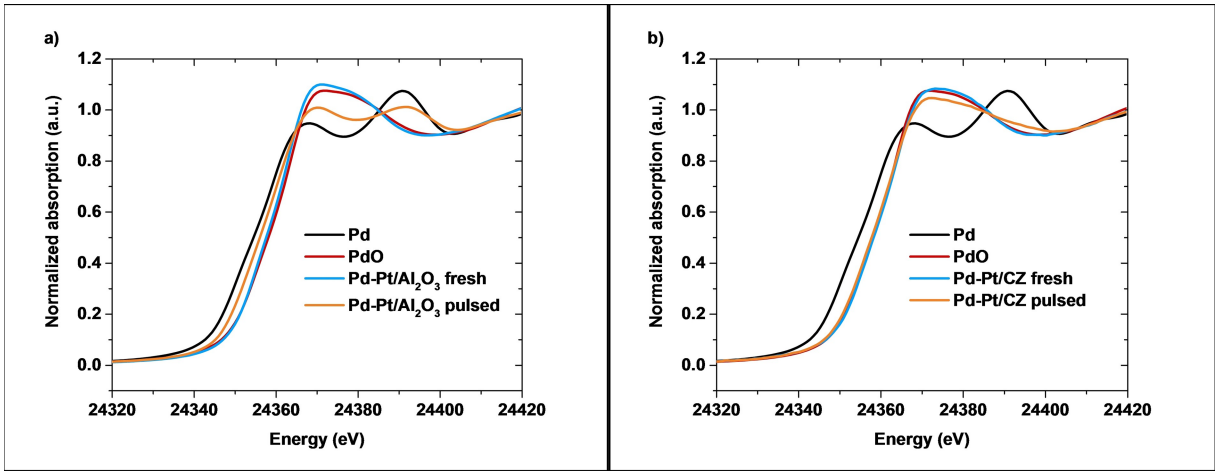

Figure 9. XANES spectra of **a)** Pd–Pt/Al_2O_3 and **b)** Pd–Pt/CZ, both in fresh state and after 4 h of H_2/O_2 pulsing at 315 °C and the references Pd and PdO.

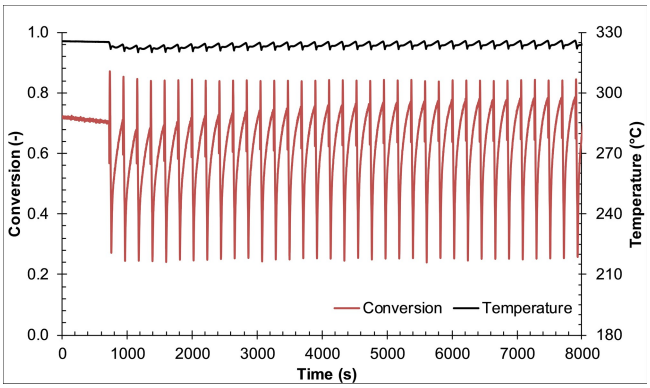

Figure 10. Effluent CH_4 conversion and temperature for Pd–Pt/CZ in 2000 ppm CH_4, bal. Ar with 30 s/180 s of 0% O_2/10% O_2 at 315 °C.

are needed, including more advanced methods such as isotopically labelled experiments. Finally, we believe that these CZ support effects explain why Pd–Pt/Al_2O_3 exhibits a higher degree of metallic Pd and subsequent increased CH_4 oxidation activity. The increased mobility of lattice oxygen of the CZ support allows either the easy reoxidation of metallic Pd to PdO or hinders the reduction of PdO to metallic Pd in the first place when compared to a support such as Al_2O_3.

Effect of pulses: O_2 pulses. A single experiment was carried out at 315 °C wherein H_2 was shut-down completely and O_2 was pulsed over the catalyst. Under these dry conditions, CH_4 became a reducing agent for 30 s. Figure 10 shows the long-term pulse behavior of the Pd–Pt/CZ catalyst during these pulses. Under O_2 pulses, CH_4 oxidation was stabilized between 85% and 30%. While these bounds remained constant through the pulses, sharper activity changes were observed as O_2 turned on and off – catalytic activity decreased faster during the reductive CH_4 pulse and rose higher when gaseous O_2 returned as the experiment progressed. This activity was balanced out by a sharp increase in activity – similar to the spike seen under wet H_2/O_2 pulsing at 400 °C (Figure S9b) – that decreased as time went on. This experiment suggests that the strength of H_2 as a reductive agent plays a role at least in the low temperature range in the improvements seen during H_2/O_2 pulsing experiments, but that some benefits can be obtained from weaker reducing agents or simply shutting off O_2 periodically.

Conclusions

While in the lively debate concerning the active phase of Pd during methane oxidation a consensus has formed around PdO as the active phase under typical lean conditions, recent research has suggested that some amounts of metallic Pd might possibly boost catalytic activity. Our research joins the latter corpus of work and suggests a process controlled increase in methane oxidation activity. *In situ* pulses of H_2 reversed catalytic deactivation of bimetallic Pd–Pt methane oxidation catalysts and maintained high activity over several hours that persisted into future experiments. The presence of H_2O resulted in a much higher methane oxidation activity during the rich pulse while methane activity dropped to zero under dry conditions. XAS revealed exclusively PdO on fresh samples, while a combination of metallic Pd and PdO was found for samples after pulsing. This suggests that a metastable PdO–Pd structure is the predominant cause behind the increased activity of pulsed catalysts, either due to an enhanced activity via the Mars-van-Krevelen mechanism or because the formed Pd–PdO species is less prone to water poisoning. Moreover, pulse-induced removal of surface hydroxyl species and the formation of lattice oxygen vacancies contribute to the increased activity. Pd–Pt/Al_2O_3 had a higher concentration of alloyed Pd–Pt and a higher percentage of metallic Pd after pulsing, resulting in a larger shift in light-off temperature compared to pulsed Pd–Pt/CZ samples.

The effects of H_2 were also dependent upon the gas environment of the catalyst. In the presence of constant O_2 flow, pulses of additional H_2 reacted over the Pd to form H_2O, resulting in a high temperature region at the front of the catalyst. Under dry conditions, the inhibition due to the H_2O negated the improvements from the increased temperature. Under wet conditions modest improvements were observed as the catalyst was already saturated. Under steady-state conditions, however, the raised catalytic temperature promoted the activity, resulting in light-off curves significantly shifted to lower temperatures.

Experiments varying the pulse durations of H_2/O_2 switching revealed that the beneficial effects could still be obtained with shorter reductive pulses and longer oxidative periods. An experiment with O_2 on/off pulsing showed that CH_4 could stabilize catalytic activity to a lesser degree than H_2 pulsing accomplished. Future experiments concerning the strength of different reductive agents as well as the duration and frequency of reductive pulses could result in an optimized method for maintaining high methane oxidation under wet conditions at low operating temperatures, which is a key step in making natural gas processes sustainable and competitive.

Experimental Section

Powder catalyst samples were prepared by incipient wetness impregnation of Al_2O_3 or CeO_2-ZrO_2-Y_2O_3-La_2O_3 using tetraammineplatinum(II)nitrate and tetraamminepalladium(II)nitrate as precursors. After coating cordierite substrates with the received powder, the monolith samples were tested under model exhaust gas conditions in a quartz glass tubular reactor. For spatially resolved experiments the setup could be equipped with a movable thin thermocouple or a thin capillary connected to a mass spectrometer (HPR-20, Hiden Analytical) placed within one of the monolith's middle channels. For all experiments, also during spatially resolved experiments, the end-of-pipe gas composition was analyzed with an MG2030 FTIR (MKS). TEM data were obtained at the LEM (KIT, Germany) using an FEI OSIRIS ChemiSTEM microscope and Pd K-edge XAS data were obtained in transmission mode at the ROCK beamline (SOLEIL, France). Comprehensive experimental details are provided in the Supporting Information.

Acknowledgements

We acknowledge A. Deutsch (ITCP, KIT) for the BET-measurements and H. Störmer (LEM, KIT) for TEM measurements. We acknowledge SOLEIL for provision of synchrotron radiation facilities and we would like to thank S. Belin and V. Briois for assistance in using beamline ROCK. This work was supported by a public grant overseen by the French National Research Agency (ANR) as part of the "Investissements d'Avenir" program (reference ANR-10-EQPX-45). We acknowledge M. Casapu (ITCP, KIT) for her support during the beamtime and fruitful discussion. K. Karinshak gratefully thanks the German Fulbright Commission, the Germanistic Society of America and the Alfried Krupp von Bohlen und Halbach Foundation for financial support, P. Lott gratefully thanks the "Fonds der Chemischen Industrie" (FCI) and the Karlsruhe House of Young Scientists (KHYS) for financial support.

Conflict of Interest

The authors declare no conflict of interest.

Keywords: methane oxidation · palladium · emission control · heterogeneous catalysis · spatial resolution technique

[1] O. Boucher, P. Friedlingstein, B. Collins, K. P. Shine, *Environ. Res. Lett.* **2009**, *4*, 044007.
[2] O. Deutschmann, J.-D. Grunwaldt, *Chem. Ing. Tech.* **2013**, *85*, 595–617.
[3] P. Gélin, M. Primet, *Appl. Catal. B* **2002**, *39*, 1–37.
[4] D. Ciuparu, M. R. Lyubovsky, E. Altman, L. D. Pfefferle, A. Datye, *Catal. Rev. Sci. Eng.* **2002**, *44*, 593–649.
[5] H. Xiong, M. H. Wiebenga, C. Carrillo, J. R. Gaudet, H. N. Pham, D. Kunwar, S. H. Oh, G. Qi, C. H. Kim, A. K. Datye, *Appl. Catal. B* **2018**, *236*, 436–444.
[6] J. Nilsson, P. A. Carlsson, N. M. Martin, E. C. Adams, G. Agostini, H. Grönbeck, M. Skoglundh, *J. Catal.* **2017**, *356*, 237–245.
[7] D. Ciuparu, L. Pfefferle, *Catal. Today* **2002**, *77*, 167–179.
[8] H. Stotz, L. Maier, A. Boubnov, A. T. Gremminger, J.-D. Grunwaldt, O. Deutschmann, *J. Catal.* **2019**, *370*, 152–175.
[9] P. Lott, P. Dolcet, M. Casapu, J.-D. Grunwaldt, O. Deutschmann, *Ind. Eng. Chem. Res.* **2019**, *58*, 12561–12570.
[10] S. K. Matam, M. H. Aguirre, A. Weidenkaff, D. Ferri, *J. Phys. Chem. C* **2010**, *114*, 9439–9443.
[11] A. Hellman, A. Resta, N. M. Martin, J. Gustafson, A. Trinchero, P. A. Carlsson, O. Balmes, R. Felici, R. van Rijn, J. W. M. Frenken, J. N. Andersen, E. Lundgren, H. Grönbeck, *J. Phys. Chem. Lett.* **2012**, *3*, 678–682.
[12] M. Lyubovsky, L. Pfefferle, *Catal. Today* **1999**, *47*, 29–44.
[13] K. Persson, K. Jansson, S. G. Järås, *J. Catal.* **2007**, *245*, 401–414.
[14] G. W. Graham, D. König, B. D. Poindexter, J. T. Remillard, W. H. Weber, *Top. Catal.* **1999**, *8*, 35–43.
[15] J. Nilsson, P.-A. Carlsson, S. Fouladvand, N. M. Martin, J. Gustafson, M. A. Newton, E. Lundgren, H. Grönbeck, M. Skoglundh, *ACS Catal.* **2015**, *5*, 2481–2489.
[16] J. Au-Yeung, K. Chen, A. T. Bell, E. Iglesia, *J. Catal.* **1999**, *188*, 132–139.
[17] C. A. Müller, M. Maciejewski, R. A. Koeppel, A. Baiker, *Catal. Today* **1999**, *47*, 245–252.
[18] A. Gremminger, P. Lott, M. Merts, M. Casapu, J.-D. Grunwaldt, O. Deutschmann, *Appl. Catal. B* **2017**, *218*, 833–843.
[19] G. S. Bugosh, V. G. Easterling, I. A. Rusakova, M. P. Harold, *Appl. Catal. B* **2015**, *165*, 68–78.
[20] C. Bozo, N. Guilhaume, J.-M. Herrmann, *J. Catal.* **2001**, *203*, 393–406.
[21] J. B. Miller, M. Malatpure, *Appl. Catal. A* **2015**, *495*, 54–62.
[22] A. T. Gremminger, H. W. Pereira de Carvalho, R. Popescu, J.-D. Grunwaldt, O. Deutschmann, *Catal. Today* **2015**, *258*, 470–480.
[23] P. Lott, M. Eck, D. E. Doronkin, R. Popescu, M. Casapu, J.-D. Grunwaldt, O. Deutschmann, *Top. Catal.* **2019**, *62*, 164–171.
[24] K. Persson, A. Ersson, K. Jansson, J. L. G. Fierro, S. G. Järås, *J. Catal.* **2006**, *243*, 14–24.
[25] G. Lapisardi, L. Urfels, P. Gélin, M. Primet, A. Kaddouri, E. Garbowski, S. Toppi, E. Tena, *Catal. Today* **2006**, *117*, 564–568.
[26] P. Castellazzi, G. Groppi, P. Forzatti, *Appl. Catal. B* **2010**, *95*, 303–311.
[27] N. M. Kinnunen, J. T. Hirvi, M. Suvanto, T. A. Pakkanen, *J. Mol. Catal. A* **2012**, *356*, 20–28.
[28] K. Narui, H. Yata, K. Furuta, A. Nishida, Y. Kohtoku, T. Matsuzaki, *Appl. Catal. A* **1999**, *179*, 165–173.
[29] A. Ersson, H. Kušar, R. Carroni, T. Griffin, S. Järås, *Catal. Today* **2003**, *83*, 265–277.
[30] Y. Ozawa, Y. Tochihara, A. Watanabe, M. Nagai, S. Omi, *Appl. Catal. A* **2004**, *259*, 1–7.
[31] M. S. Wilburn, W. S. Epling, *Appl. Catal. B* **2017**, *206*, 589–598.
[32] W. S. Epling, G. B. Hoflund, *J. Catal.* **1999**, *182*, 5–12.
[33] Y.-H. (Cathy) Chin, M. García-Diéguez, E. Iglesia, *J. Phys. Chem. C* **2016**, *120*, 1446–1460.
[34] N. Sadokhina, F. Ghasempour, X. Auvray, G. Smedler, U. Nylén, M. Olofsson, L. Olsson, *Catal. Lett.* **2017**, *147*, 2360–2371.
[35] L. S. Escandón, D. Niño, E. Díaz, S. Ordóñez, F. V. Díez, *Catal. Commun.* **2008**, *9*, 2291–2296.
[36] D. Ciuparu, F. Bozon-Verduraz, L. Pfefferle, *J. Phys. Chem. B* **2002**, *106*, 3434–3442.
[37] D. Ciuparu, E. Perkins, L. Pfefferle, *Appl. Catal. A* **2004**, *263*, 145–153.
[38] F. Arosio, S. Colussi, G. Groppi, A. Trovarelli, *Catal. Today* **2006**, *117*, 569–576.
[39] N. Ottinger, R. Veele, Y. Xi, Z. G. Liu, *SAE Int. J. Engines* **2015**, *8*, 2015-01–0991.
[40] A. W. Petrov, D. Ferri, F. Krumeich, M. Nachtegaal, J. A. Van Bokhoven, O. Kröcher, *Nat. Commun.* **2018**, DOI 10.1038/s41467-018-04748-x.
[41] D. Bounechada, G. Groppi, P. Forzatti, K. Kallinen, T. Kinnunen, *Top. Catal.* **2013**, *56*, 372–377.
[42] A. K. Datye, J. Bravo, T. R. Nelson, P. Atanasova, M. Lyubovsky, L. Pfefferle, *Appl. Catal. A* **2000**, *198*, 179–196.
[43] R. Kikuchi, S. Maeda, K. Sasaki, S. Wennerström, K. Eguchi, *Appl. Catal. A* **2002**, *232*, 23–28.
[44] W. Barrett, J. Shen, Y. Hu, R. E. Hayes, R. W. J. Scott, N. Semagina, *ChemCatChem* **2020**, *12*, 944–952.
[45] Y. Mahara, K. Murata, K. Ueda, J. Ohyama, K. Kato, A. Satsuma, *ChemCatChem* **2018**, *10*, 3384–3387.

Manuscript received: April 7, 2020
Accepted manuscript online: April 13, 2020
Version of record online: June 8, 2020